Mon. Not. R. Astron. Soc. **000**, 1–?? (2005) Printed 25 August 2014 (MN LATEX style file v2.2)

Chemical evolution of galaxies with radiation-driven dust wind

arXiv:1408.5197v1 [astro-ph.GA] 22 Aug 2014

Kenji Bekki[1⋆] and Takuji Tsujimoto[2]
[1]*ICRAR M468 The University of Western Australia 35 Stirling Hwy, Crawley Western Australia 6009, Australia*
[2]*National Astronomical Observatory of Japan, Mitaka-shi, Tokyo 181-8588, Japan*

Accepted, Received 2005 February 20; in original form

ABSTRACT
We discuss how the removal of interstellar dust by radiation pressure of stars influences the chemical evolution of galaxies by using a new one-zone chemical evolution models with dust wind. The removal efficiency of an element (e.g., Fe, Mg, and Ca) through radiation-driven dust wind in a galaxy is assumed to depend both on the dust depletion level of the element in interstellar medium and the total luminosity of the galaxy in the new model. We particularly focus on the time evolution of [α/Fe] and its dependence on model parameters for dust wind in this study. The principal results are as follows. The time evolution of [Ca/Fe] is significantly different between models with and without dust wind in the sense that [Ca/Fe] can be systematically lower in the models with dust wind. The time evolution of [Mg/Fe], on the other hand, can not be so different between the models with and without dust wind owing to the lower level of dust depletion for Mg. As a result of this, [Mg/Ca] can be systematically higher in the models with dust wind. We compare these results with the observed elemental features of stars in the Large Magellanic Cloud (LMC), because a growing number of observational studies on [α/Fe] for the LMC have been recently accumulated for a detailed comparison. Based on the present new results, we also discuss the origins of [α/Fe] in the Fornax dwarf galaxy and elliptical galaxies in the context of radiation-driven dust wind.

Key words: galaxies:abundances – galaxies:ISM – galaxies:evolution – ISM: dust, extinction – stars:formation

1 INTRODUCTION

Interstellar dust is a fundamentally important component of interstellar medium (ISM) in galaxies, because it can control interstellar chemistry of variously different elements, drive the formation of molecular hydrogen, and modify the spectral energy distributions of galaxies through absorption and emission of stellar light. Dust can form from gas and metals ejected from supernovae (SNe) and Asymptotic giant branch (AGB) stars, grow through accretion of metals onto pre-existing grains, and be destroyed by a number of physical processes such as SN explosions and shocks (e.g., Jones et al. 1995; See Hirashita 2013 for a recent review on physical processes related to dust evolution). Therefore, the time evolution of star formation rates and physical conditions of ISM can cause rather complicated evolution processes of dust in galaxies. Although the complicated evolution processes of dust in galaxies have been investigated both by one-zone chemical evolution models (e.g., Dwek 1998) and numerical simulations (e.g., Bekki 2013; Yozin & Bekki 2014), they are yet to be fully understood.

Radiation pressure of stars has long been considered to be one of key physical processes of dust evolution in galaxies (e.g., Chiao & Wickramasinghe 1972; Barsella et al. 1989; Ferrara et al.1991, F91; Aguirre et al. 2001). Radiation pressure of stars on dust grains is demonstrated to cause dust wind in star-forming disk galaxies and the dust wind can be responsible both for the formation of the dusty halos around galaxies and for the origin of intergalactic dust (e.g., F91). Such efficient removal of dust from galaxies through radiation-driven wind could cause significant changes of chemical abundance pattern in galaxies owing to the observed different levels of dust depletion among different chemical elements (e.g., no depletion for N and severe depletion for Ca). One of obvious effects of dust removal on galaxy evolution is that the formation efficiency of H_2 can be significantly lowered by the reduced amount of dust in ISM.

Chemical evolution of galaxies should be strongly influenced by the removal of dust through radiation-driven dust

⋆ E-mail: bekki@cyllene.uwa.edu.au

wind, because a large fraction of metal is observed to be locked up in dust of ISM (e.g., Savage & Sembach 1996, SS96; Draine 2009; Jenkins 2009). However, previous one-zone chemical evolution models with dust formation and destruction did not consider this important effect of radiation-driven dust wind on chemical evolution (e.g., Dwek 1998; Hirashita 1999; Calura et al. 2008; Pipino et al. 2010). Recent chemodynamical models of galaxy formation with dust evolution did not incorporate the radiation pressure of stars on dust grains in a self-consistent manner (Bekki 2013, 2014), though dust removal through supernova wind is included. Therefore, it is largely unclear how the dust wind by radiation pressure of stars can influence the chemical evolution of galaxies.

A growing number of observational studies have revealed some evidences for the existence of dust far beyond galactic disks and for the outflow of dust in actively star-forming galaxies (e.g., Holwerda et al. 2009; Roussel et al. 2010; Ménard et al. 2010; Yoshida et al. 2011; Peek et al. 2013). For example, Ménard et al. (2010) detected the presence of dust at $R \sim 20$ kpc to several Mpc by investigating the correlations between the brightness of ~ 85000 quasars and the positions of $\sim 2.4 \times 10^6$ galaxies. They also found that (i) the cosmic dust density is $\Omega_{\rm dust} \sim 5 \times 10^{-6}$ and (ii) roughly the half of the cosmic dust can come from dust in the halos of luminous ($L \sim L^*$) galaxies. The observed large amount of dust in galaxy halos strongly suggests that dust removal from the main bodies of galaxies needs to be seriously considered in theoretical models of dust and metal evolution in galaxies.

Recently Pompéia et al. 2008 (P08) investigated [α/Fe] of stars in the Large Magellanic Cloud (LMC) and found that [Ca/Fe] is significantly (by 0.2−0.4 dex) underabundant in comparison with other [α/Fe] (e.g., [Mg/Fe]). Although Bekki & Tsujimoto (2012, BT12) have tried to reproduce the observed very low [Ca/Fe] and almost solar [Mg/Fe] in the LMC by using their chemical evolution models with canonical IMFs, they have failed to reproduce such unique chemical abundances of the LMC. They have therefore concluded that some physical processes which can lead to the selective removal of Ca would be required for explaining self-consistently both the observed [Mg/Ca] and [Ca/Fe] of the LMC stars. Furthermore, unusually low [Ca/Fe] has been observed for the stars in the Fornax dwarf galaxy (e.g., Letarte et al. 2010). If these low [Ca/Fe] in massive dwarf galaxies are real, then the origin needs to be clarified by theoretical models of galaxy formation and evolution.

The purpose of this paper is thus to construct a new chemical evolution model with radiation-driven dust wind and thereby to discuss how the dust removal from galaxies can influence galactic chemical evolution. We particularly focus on the influences of dust wind on the evolution of [α/Fe], because the observed dust depletion levels of these α elements are quite different with one another (e.g., SS96). We compare the results of our new models mainly with the corresponding observations for the LMC in the present study, firstly because our previous models (BT12) failed to explain the observed [Ca/Fe]-[Fe/H] and [Mg/Fe]-[Fe/H] relations self-consistently by using a canonical model without dust wind, and secondly because a growing number of observations have been accumulated for the LMC that can allow us to make a detailed comparison between observations and models (e.g., Colucci et al. 2012, C12; Haschke et al. 2012; Van der Swaelmen et al. 2013, V13).

The plan of the paper is as follows: In the next section, we describe our new one-zone chemical evolution models with radiation-driven dust wind. In §3, we present the results on the [α/Fe] evolution and its dependence on model parameters for dust wind. In this section, we particularly discuss correlations between [Mg/Ca] and [Fe/H] in the models with and without dust wind. In §4, we discuss the latest observational results on the [Ca/Fe]-[Fe/H] relations of the Fornax dwarf galaxy and lower [Ca/Fe] in elliptical galaxies. We summarize our conclusions in §5. Although there are numerous key papers on chemical evolution models of galaxies with different types (e.g., Matteucci & Francois 1989; Pagel & Tautvaišienė 1998; Lanfranchi & Matteucci 2010; Kirby et al. 2011; Tsujimoto & Bekki 2012), we do not discuss each of these in detail, because it is simply beyond the scope of this paper. We do not discuss the origin of intriguing chemical abundances of dwarfs (Sgr and ultra-faint dwarfs, e.g., McWilliam et al. 2013; Roederer & Kirby 2014) other than the LMC and Fornax either in this paper.

2 THE MODEL

2.1 Outline

This paper describes our first attempt to investigate the possible influences of radiation-driven dust wind on galactic chemical evolution. We therefore adopt a rather idealized one-zone chemical evolution model in order to demonstrate such influences more clearly. The present study adopts the following big picture of dust removal processes in galaxies. First, gas and dust mostly in cool ISM can be expelled from disk to halo regions of a galaxy through energetic stellar winds and radiation pressure of stars on dust grains. At this stage, dust and gas may or may not be hydrodynamically coupled with each other depending on the gas densities of the ejected matter and the relative velocity of gas and dust. Then radiation pressure on dust can expel only the dust further from the halo region so that dust can be completely removed from the galaxy and thus can not be recycled into the original ISM. This removal process of metals through dust wind is different in different heavy elements (Mg, Ca, and Fe) so that the time evolution of chemical abundance patterns can be significantly influenced by the removal process.

The present one-zone model adopts three assumptions on (i) from where dust can be removed more efficiently in gas disks (e.g., from cool or warm ISM), (ii) whether dust and gas dynamics can be coupled with each other, and (iii) how the removal processes of heavy metals (e.g., Mg, Ca, and Fe) can depend on the depletion levels and sizes of dust containing the metals, and they are described below in §2.1.1-3. The present big picture of the dust removal process from galaxies is based on the three assumptions in the present study. We admit that the present models might be less realistic in some points owing to these assumptions, but we consider that the present models are reasonable enough to grasp some essential influences of dust wind on chemical evolution of galaxies in this first investigation. More sophisticated models for dust removal processes should be constructed in our future studies.

2.1.1 Efficient dust removal from cool ISM

We assume that a much larger amount of dust can be removed from cool ISM rather than warm and hot ISM in a galaxy. This assumption is quite reasonable as follows. Previous observations revealed that dust depletion for heavy elements (Fe, Mg, and Ca) is much more severe in cool ISM than in warm and hot ISM (e.g., Welty et al. 1999). For example, the Ca-depletion level in cool ISM is ~ 16 times greater than that in warm ISM (See Fig. 6 in Welty et al. 1999). Furthermore, the typical hydrogen number fraction per unit volume ($f_{\rm H} \propto f_{\rm V} n_{\rm H}$, where $f_{\rm V}$ and $n_{\rm H}$ are the volume filling factor and hydrogen number density at each phase, respectively) in the hot, warm, and cool (cool and diffuse H_2 and cool H I) are 0.002, 0.2, and 0.6 cm^{-3}, respectively (Drain 2009). These observations mean that the vast majority of heavy metals (that are relevant to the present study) are locked up in dust of cool ISM. In the three-component ISM (McKee & Ostriker 1977), the total mass of metals removed from a galaxy ($\delta M_{\rm metal}$) through dust wind can be given as follows:

$$\delta M_{\rm metal} \propto \delta (M_{\rm dust,hot} + M_{\rm dust,warm} + M_{\rm dust,cool}), \quad (1)$$

where $M_{\rm dust,hot}$, $M_{\rm dust,warm}$, and $M_{\rm dust,cool}$ are the total dust masses in hot, warm, and cool ISM, respectively. By considering the above observations, we assume that

$$\delta M_{\rm metal} \propto \delta M_{\rm dust,cool}. \quad (2)$$

We accordingly use the observed dust depletion patterns of individual elements (e.g., Mg and Ca) for cool ISM in order to estimate the total amount of metals that are locked up in dust and can be thus removed from a galaxy through radiation-driven dust wind. The adopted dust depletion levels for the investigated elements in this study is summarized in Table 1. The detailed model for this dust removal process is given later in §2.3.

Since depletion levels are rather high in cool ISM and they are quite different between different elements, selective removal of dust from cool ISM can influence galactic chemical evolution and thus is worthy of a detailed investigation. However, even if dust is removed selectively from warm and hot ISM, such removal can not influence the time evolution of abundance patterns in galaxies significantly owing to the rather low depletion levels and the smaller element-to-element differences in the depletion levels. An idealized model for the adopted selective loss of dust from cool ISM is presented later in this paper.

2.1.2 Dust-gas decoupling in galactic halos

We assume that only dust can be removed completely from a galaxy (i.e., from its halo) through radiation pressure of stars for some physical conditions so that dust can not be recycled later into ISM of the galaxy (i.e., gas can not be escaped from the galaxy). This assumption can be reasonable and realistic as follows. Many authors have already investigated physical conditions for dust-gas hydrodynamical coupling in galaxies (e.g., Spitzer 1978; Franco et al. 1991; F91; Davies et al. 1998), and found that dust-gas coupling is possible in the relatively high-density part of ISM in galaxies. For example, Franco et al. (1991) shows that gas clouds can be transferred to high latitudes in the Galaxy, because radiation pressure on dust grains can raise both the dust and gas above the gas disk owing to the dust-gas coupling ('photolevitation process').

However, F91 demonstrated that after dust can be located above the disk owing to the photolevitation process, the dust can be further expelled by radiation wind from a galaxy (depending on several parameters though). These previous theoretical models suggested that dust can be selectively removed from galaxies to become intergalactic dust, though the final states of dust depend strongly on the details of their models. More recently, Murray et al. (2005) and Coker et al. (2013) discussed dust-gas coupling in galaxies and found that dust-gas coupling can be important on galaxy-scale gas dynamics such as dust wind evolution only if ISM density can be as high as or higher than $0.01 - 0.1$ cm^{-3}. This means that in the low-density halo regions (less than $\sim 10^{-4} - 10^{-5}$ cm^{-3} for the Galaxy, e.g., Sembach et al. 2003) of galaxies, gas and dust should be dynamically decoupled. It is therefore highly likely that only dust can escape from galaxies (if radiation pressure is strong enough) after both dust and gas have reached the halo regions.

The assumed selective removal of dust is consistent with recent observational results by Xilouris et al. (2006), who found a very large dust-to-gas-ratio ($D \sim 0.05$, which is about 6 times larger than the solar neighborhood) in the outer halo of M81. This can not be explained if both gas and dust are removed equally from galaxies in M81 group and later located in the outer halo region of M81. The observed very large dust-to-gas ratio can be explained, if dust can be much more efficiently removed from galaxies than gas to reach the outer halo region of M81 finally. Furthermore, such selective removal of dust from galaxies appears to be consistent with a recent observation that about 50% of all dust is located in outer halo regions (at $R \sim 20$ kpc to several Mpc) of luminous galaxies (Ménard et al. 2010). We therefore consider that much more efficient removal of dust from galaxies (in comparison with gas) is quite reasonable and realistic (i.e., consistent with observations) in the present study.

2.1.3 Dust removal efficiencies dependent on dust depletion levels

As shown by F91, the dust removal efficiencies depend on dust sizes for a given time-dependent radiation field of stars in a galaxy. Therefore, if dust sizes are different between different dust populations (e.g., Mg-bearing and Ca-bearing dust), then the removal efficiencies could be different between them. Since we do not have enough observational details on the size/composition differences in different dust populations, we can not currently construct a realistic model for dust size distributions for individual dust populations based on observations.

Theoretical models on dust properties of stars have provided dust compositions just for a number of key individual dust populations (e.g., $MgSiO_4$, MgO, Al_2O_3, and FeS) in AGB stars and SNe (e.g., Nozawa et al. 2003; Piovan et al. 2011). Since the detailed information on the size distributions of Mg- and Ca-bearing dust (that are important in the present study) have not been provided yet, we can not currently investigate the possible differences in dust removal efficiencies between different dust populations (owing to dif-

ferent responses of dust to radiation field between these dust caused by their different size distributions and compositions) in a quantitative manner. However, we can discuss the possible differences in the sizes between Mg- and Ca-bearing dust based on some results of recent theoretical works on dust size distributions.

Nozawa et al. (2003) investigated the dust size distributions produced by SNe with different masses for a number of dust population (e.g., Mg_2SiO4 and FeS) and found that the typical dust sizes range from $2 \times 10^{-4} \mu$m to $10^{-1} \mu$m (See their Fig. 10). The dust produced by AGB stars are demonstrated to have size distributions biased toward the larger size of $\sim 0.1 \mu$m (e.g., Winters et al. 1997; Yasuda & Kozasa 2012). These theoretical results suggest that the typical size of SNe dust is significantly smaller than that of AGB dust.

Mg-bearing dust is demonstrated to be formed efficiently both in AGB stars (e.g., Ferrarotti & Gail 2006) and SNe (e.g., Nozawa et al. 2003) while the formation efficiency of Ca-bearing dust ($CaCO_3$) is suggested to be negligibly small in AGB stars (Ferrarotti & Gail 2005). Therefore, if Ca-bearing dust can be more preferentially formed in SNe, the above theoretical results by Nozawa et al. (2003) and Winters et al. (1997) would imply that the typical size of Ca-bearing dust can be smaller than that of Mg-bearing dust. If the sizes of Ca-bearing dust are really systematically smaller than those of Mg-bearing dust, then the Ca-bearing dust can be more efficiently removed from a galaxy for a given radiation field of stars in the galaxy, because smaller dust grains can be more efficiently removed from galaxies by radiation pressure (F91).

It should be stressed, however, that the later evolution of dust by destruction processes of SNe and dust coagulation processes in ISM can significantly change the dust size distributions (e.g., Hirashita & Yan 2009). It is therefore reasonable for us to consider that we simply do not know the typical sizes of Mg- and Ca-bearing dust in real ISM. It is ideal that we can adopt a model in which the removal efficiency of a (i-th) metal element (ϵ_i) through dust wind for a given radiation field depends both on the typical size of dust containing the element (λ_i) and the dust depletion level of the element (δ_i) as follows:

$$\epsilon_i = F(\lambda_i, \delta_i), \tag{3}$$

where the functional form (F) should be modeled properly. However, owing to the lack of observational and theoretical works on λ_i for heavy elements relevant to the present work (e.g., Mg, Ca, and Fe), we can not include the dependences of ϵ_i on λ_i in the present study and thus we assume that ϵ_i depends solely on δ_i as follows:

$$\epsilon_i = F(\delta_i). \tag{4}$$

We admit that this model is oversimplified to some extent and thus suggest that the present results could be changed if a realistic model for the influences of the typical sizes of different dust populations on dust removal efficiencies is included. We briefly discuss the possible influences of dust size differences on the present results later in §4.1.

Thus we here assume that the removal efficiency of an element through dust wind depends solely on the dust depletion level for a given radiation field of a galaxy. The details of the model are given later in §2.3. For the adopted model, a larger mass fraction of Ca is locked up in dust (than Mg) so that a larger amount of Ca metal can be efficiently removed from a galaxy through dust wind than Mg. This is quite reasonable, because Ca in cool ISM of the Galaxy is observed to be more severely dust-depleted than Mg (i.e., a larger amount of metal is locked up in dust for Ca). However, it should be noted that we do not know direct evidence for this more efficient loss of Ca in real galaxies. What we can do in this paper is to investigate in what models for dust removal efficiencies the observed abundance patterns of galaxies can be better reproduced. We thus fully admit that there would be an uncertainty in the present model for the possibly different dust removal efficiencies between different elements.

Table 1. The depletion level (δ_i) for the selected four elements.

Element [a]	δ_i [b]
Mg	1.1×10^{-1}
Ca	1.7×10^{-4}
Fe	3.7×10^{-3}
Ti	1.0×10^{-3}

[a] The time evolution of these four elements are investigated in detail by the present one-zone chemical evolution models.
[b] These values are calculated for the data given in SS96 and Draine 2009. The smaller δ_i for the i-th element means that a larger amount of the element is locked up in dust grains.

Table 2. Model parameters for one-zone chemical evolution.

Model [a]	β [b]	γ [c]	$C_{\rm r}$ [d]
M1	...	...	...
M2	0	-1	10^{-3}
M3	0.1	-1	10^{-3}
M4	0.3	-1	10^{-3}
M5	0.5	-1	10^{-3}
M6	0.3	-0.5	10^{-3}
M7	0.3	-0.3	10^{-3}
M8	0.1	-0.5	10^{-3}
M9	0.1	-0.3	10^{-3}
M10	0	-0.5	10^{-3}
F1	...	...	...
F2	0	-1	6×10^{-3}
E1	...	...	...
E2	0	-1	10^{-3}
E3	0	-1	7×10^{-4}
E4	0	-1	3×10^{-4}

[a] The 'M', 'F', and 'E' are referred to as the Magellanic Clouds (LMC), Fornax, and Early-type galaxy models, respectively. The models with no values of β, γ, and $C_{\rm r}$ indicated (e.g., M1 and F1) are those without dust wind.
[b] The parameter that controls dust removal fraction and defines the minimum level of dust removal.
[c] The parameter that controls dust removal fraction and determine the degree of differential dust removal among different elements.
[d] The parameter that controls the strength of radiation pressure of stars on dust grains.

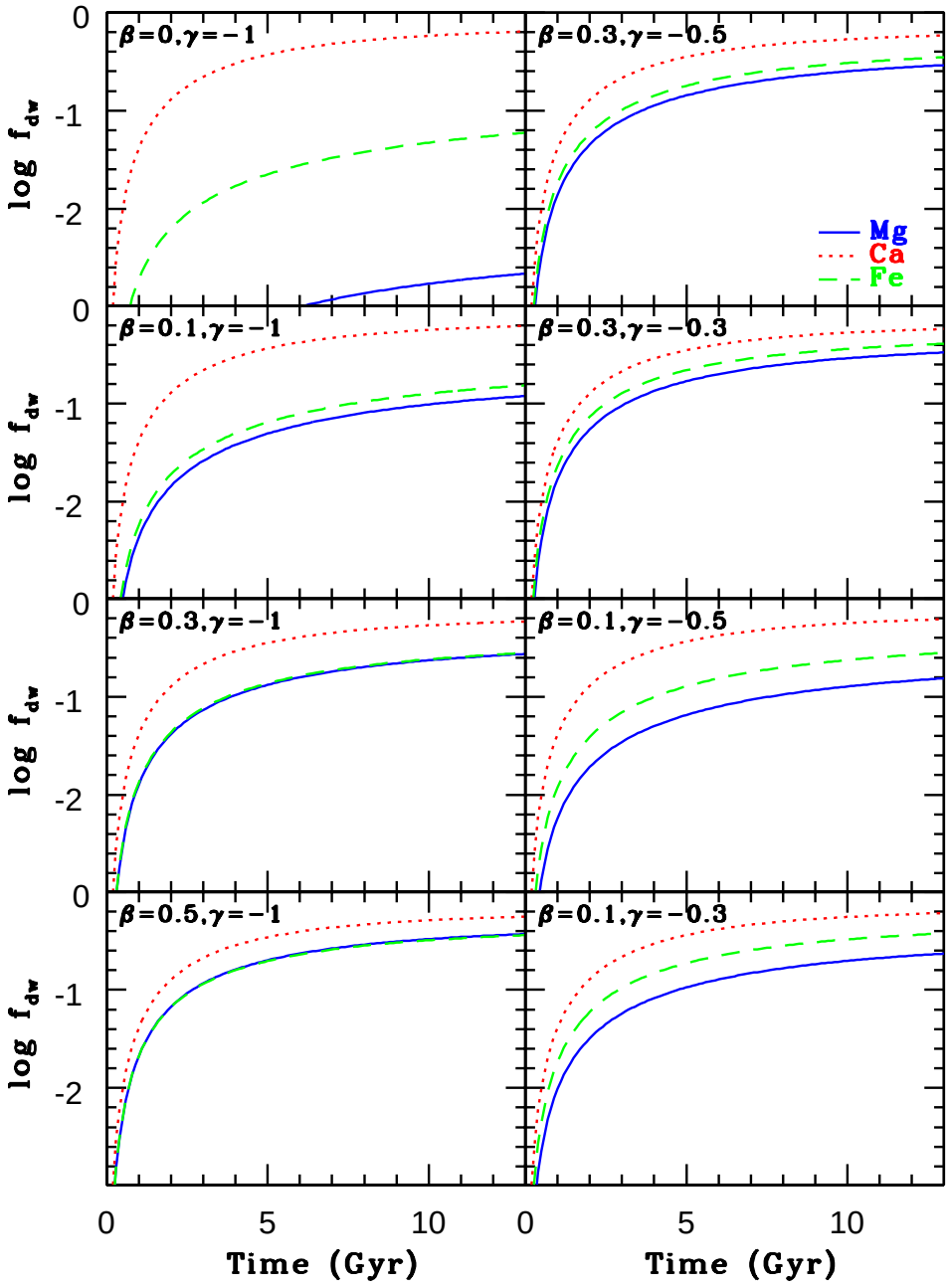

Figure 1. The time evolution of dust removal fraction ($f_{\rm dw,}i$) for i = Mg (blue solid), Ca (red dotted), and Fe (green short-dashed) in the LMC dust wind models with different β and γ indicated in the upper left panel of each frame. The larger $f_{\rm dw,}i$ means that a larger fraction of dust (thus metal) is removed from the main body of a galaxy through radiation-driven dust wind.

2.2 Basic equations

We adopt one-zone chemical evolution models that are essentially the same as those adopted in our previous studies on the chemical evolution of the LMC (BT12). Accordingly, we briefly describe the adopted models in the present study. A galaxy is assumed to form through a continuous gas infall from outside the disk region (e.g., halo) for $0 \leqslant t \leqslant t_{\rm end}$, where $t = 0$ is the starting time of a calculation. The final time $t_{\rm end}$ of a calculation is set to be 13 Gyr for most models. We investigate the time evolution of the gas mass fraction ($f_{\rm g}(t)$), the star formation rate ($\psi(t)$), and the abundance of the ith heavy element ($Z_i(t)$) for a given accretion rate ($A(t)$), IMF, ejection rate of ISM due to SNe ($w(t)$) and ejection rate of ISM due to SNe ($w_{\rm d}(t)$) *through dust wind.*

The basic equations for the adopted one-zone chemical evolution models are described as follows:

$$\frac{df_g}{dt} = -\alpha_1\psi(t) + A(t) - w(t) - w_{\rm d}(t) \qquad (5)$$

$$\frac{d(Z_i f_g)}{dt} = -\alpha_{\rm l} Z_i(t)\psi(t) + Z_{A,i}(t)A(t) + y_{{\rm II},i}\psi(t) + y_{{\rm Ia},i}\int_0^t \psi(t-t_{\rm Ia})g(t_{\rm Ia})dt_{\rm Ia} - W_i(t) - W_{{\rm d},i}(t) \ , \quad (6)$$

where $\alpha_{\rm l}$ is the mass fraction (per unit mass) locked up in dead stellar remnants and long-lived stars, $y_{\rm Ia,i}$, $y_{\rm II,i}$ are the chemical yields (per unit mass) for the ith element from type II supernovae (SN II), from SN Ia, respectively, $Z_{A,i}$ is the abundance of heavy elements contained in the infalling gas, W_i is the rate of supernova wind for each element, and $W_{{\rm d},i}$ is the dust wind rate for each element (i.e., $w_{\rm d}$ is the sum of $W_{{\rm d},i}$ for all elements). Unlike BT12, we did not include the AGB term in the equations (5) and (6), because (i) the present study does not investigate the chemical evolution of [Ba/Fe] and (ii) AGB feedbacks do not play a role in the time evolution of [Mg/Fe] and [Ca/Fe].

In the present study, the total mass of a galaxy ($M_{\rm t}$) including both gas and stars is adopted as mass units for all models and accordingly the masses of all components (e.g., gas, stars, and metals) are normalized by $M_{\rm t}$. The gas mass fraction ($f_{\rm g}$) of a galaxy is normally defined as the ratio of gas mass ($M_{\rm g}$) to $M_{\rm t}$. The dust wind rate ($w_{\rm d}$) is defined as the rate of mass ejection by radiation-driven wind per unit mass (i.e., normalized by $M_{\rm t}$). The star formation ($\psi(t)$) and accretion rates ($A(t)$) are also those per unit mass (i.e., they are normalized SFRs and accretion rates). Unlike our previous studies (BT12), we do not include the ejection of metals through stellar wind (i.e., $w(t) = 0$), mainly because we try to clearly understand the roles of dust wind in galactic chemical evolution. Furthermore, as discussed in BT12, the models with no stellar wind can reproduce the observed age-metallicity relation and chemical abundances of the LMC by choosing a reasonable IMF. All of the elements in the stellar ejecta from SNe are assumed to be returned back to ISM of galaxies immediately after SN explosions.

The above chemical yields are defined as the masses of newly synthesized metals per unit mass and thus are dimensionless quantities. The chemical abundance of an element at each time is normally defined as the ratio of the total metal mass ($M_{{\rm Z},i}$) of the element to the total gas mass ($M_{\rm g}$) at the time. Both W_i and $W_{{\rm d},i}$ are wind rates per units mass (i.e., normalized by $M_{\rm t}$). It should be stressed here again that W_i is set to be 0 for all elements so that we can discuss more clearly the roles of dust wind in galactic chemical evolution.

The quantity $t_{\rm Ia}$ represents the time delay between star formation and SN Ia explosion. The term $g(t_{\rm Ia})$ is the distribution functions of SNe Ia, and the details of which are described later in this section. Thus equation (5) describes the time evolution of the gas due to star formation, gas accretion, and dust wind. Equation 6 describes the time evolution of the chemical abundances due to chemical enrichment by supernovae and metal removal through dust wind. Unlike BT12, the present study does not investigate the chemical evolution of [Ba/Fe], and thus the AGB term in the equations used in BT12 is not included in the above equations (5) and (6).

2.3 Dust wind rate

The dust wind rate $W_{{\rm d},i}(t)$ is a function of (i) a probability (P_i) that i-th element (e.g., Mg) can be locked up in dust grains and influenced by stellar radiation and (ii) the strength of stellar radiation ($S(t)$) that can be exerted on dust grains. Therefore $W_{{\rm d},i}$ is described as follows:

$$W_{{\rm d},i}(t) = P_i S(t). \quad (7)$$

The probability P_i is assumed to depend solely on the depletion level (δ_i) for the i-th element and described as follows:

$$P_i = \beta + C_{\rm p}(1-\beta)\delta_i^{\gamma}, \quad (8)$$

where β and γ are the two basic parameters that control the dependences of P_i on δ_i and $C_{\rm p}$ is a normalization constant. In this power-law formula, the larger absolute magnitude of γ means a steeper (stronger) dependence of P_i on dust depletion levels. β defines the minimum possible $P_{\rm i}$ for each element, because β is assumed to be equal to or larger than 0.

We adopt this simplified power-law formula for P_i, because the present work is the very first study on the effects of dust wind on chemical evolution of galaxies and thus needs to demonstrate the basic dust effects more clearly. The power-law formula would make it more straightforward for us to interpret the present results of the models with different model parameters (e.g., β and γ). It should be noted here that there is currently no/little strong observation constraint on how P_i might depend on dust properties (e.g., depletion levels and dust sized etc). Therefore the adopted formula for P_i might be regarded as an arbitrary one. However, we think that we can more clearly understand the essential ingredients of the dust wind effects on galactic chemical evolution thanks to the relatively simplified formula for P_i in the present study.

The depletion level δ_i is defined as follows:

$$\delta_i = \frac{(N_{i,{\rm g}}/N_{\rm H})}{(N_i/N_{\rm H})_{\odot}}, \quad (9)$$

where $(N_{i,{\rm g}}/N_{\rm H})$ is the gas-phase abundance for the i-the element (relative to H) and $(N_i/N_{\rm H})_{\odot}$ is the corresponding solar value. Accordingly, the lower δ_i means the higher level of dust depletion. Since almost all (99.98%) of Ca is dust-depleted, the constant $C_{\rm p}$ is chosen such that P_i for Ca can be 1 for a given β and γ. In the above formula for P_i, β should range from 0 to 1 while γ should be negative. We consider that the model with $\beta = 0$ and $\gamma = -1$ can be a reasonable combination in the present study, because the dust removal efficiency is proportional to the dust depletion level. We however investigate models with different β and γ, because these two parameter are not observationally constrained. We adopt the observed values of $(N_{i,{\rm g}}/N_{\rm H})$ and $(N_i/N_{\rm H})_{\odot}$ from Table 23.1 in Draine (2009).

2.4 Radiation pressure of stars

The strength of radiation pressure of stars is assumed to be proportional to the total luminosity of a galaxy as follows:

$$S(t) = C_{\rm r}\int_0^t f_{\rm M/L}^{-1}(t-T)M_{\rm ns}(T)dT, \quad (10)$$

where $f_{\rm M/L}$ is the mass-to-light ratio (M/L) of a single stellar population (SSP) and $M_{\rm ns}(T)$ is the total mass of stars formed at $t = T$. Since the M/L of a SSP is a function of age and metallicity, we need to use a stellar population synthesis code in order to properly calculate $f_{\rm M/L}$ at each time step. Accordingly, we use the code MILES (Vazdekis et al. 2010) for the M/L estimation of all models in the present study. The parameter $C_{\rm r}$ can control how much amount of metals can be removed through radiation-driven wind, and it is fixed at 10^{-3} for most models. For this value of $C_{\rm r}$ in the LMC model later described, a significant fraction of metals can be removed so that chemical evolution can be influenced by dust wind.

2.5 Star formation and gas accretion rate

The star formation rate per unit mass ($\psi(t)$) is assumed to be proportional to the gas fraction with a constant star formation coefficient and thus is described as follows:

$$\psi(t) = C_{\rm sf} f_{\rm g}(t) \tag{11}$$

The star formation coefficient ($C_{\rm sf}$) can control the rapidity of gas consumption and $C_{\rm sf} = 0.006$ is the reasonable value for the LMC (BT12) for a given set of reasonable model parameters. For the models with $C_{\rm sf} = 0.006$, both the typical SF rate and the final total stellar mass ($M_{\rm s} = 2.7 \times 10^9 M_\odot$) observed in the LMC can be reproduced by some models (BT12). For the accretion rate, we adopt the formula in which $A(t) = C_{\rm a} \exp(-t/t_{\rm a})$ and $t_{\rm a}$ is a free parameter controlling the time scale of the gas accretion. The normalization factor $C_{\rm a}$ is determined such that the total gas mass accreted onto a galaxy can be 1 (in model units) for a given $t_{\rm a}$. We investigated models with different $t_{\rm a}$ for different three types of models later described. The initial [Fe/H] of the infalling gas is set to be -3 and we assume a SN-II like enhanced [α/Fe] ratio (e.g., [Mg/Fe]$\approx$ 0.4).

2.6 Chemical yields and delay time distribution of SN Ia

We adopt the nucleosynthesis yields of SNe II and Ia from Tsujimoto et al. 1995 (T95) to deduce $y_{{\rm II},i}$ and $y_{{\rm Ia},i}$ for a given IMF. Stars with masses larger than $8M_\odot$ explode as SNe II soon after their formation and eject their metals into the ISM. In contrast, there is a time delay ($t_{\rm Ia}$) between the star formation and the metal ejection for SNe Ia. We here adopt the following delay time distribution ($g(t_{\rm Ia})$) for 0.1 Gyr $\leqslant t_{\rm Ia} \leqslant$ 10 Gyr, which is consistent with recent observational studies on the SN Ia rate in extra-galaxies (e.g., Totani et al. 2008; Maoz et al. 2010, 2011):

$$g_{\rm Ia}(t_{\rm Ia}) = C_{\rm g} t_{\rm Ia}^{-1}, \tag{12}$$

where $C_{\rm g}$ is a normalization constant that is determined by the number of SN Ia per unit mass (which is controlled by the IMF and the binary fraction for intermediate-mass stars for the adopted power-law slope of -1). The fraction of the stars that eventually produce SNe Ia for 3–8$M_\odot$ has not been observationally determined and thus is regarded as a free parameter, $f_{\rm b}$. We mainly investigate models with different$f_{\rm b} = 0.03$ and 0.09 for three different types of models later described.

Like BT12, we use the theoretically predicted yields of SN explosions from T95 for consistency between BT12 and the present work. Accordingly, the initial [Ca/Fe] is ~ 0.24 that are slightly lower than the observed [Ca/Fe] ($0.3 \sim 0.4$) for the Milky Way (MW) halo stars. We here stress that the key conclusion on the origin of the observed low [Ca/Fe] of the LMC stars in this paper remains unchanged, if we adopt different Ca yields. We discuss this point briefly in the Appendix A by using the results of the models with different Ca yields.

2.7 IMF

The adopted IMF is defined as $\Psi(m_{\rm I}) = M_{s,0} {m_{\rm I}}^{-\alpha}$, where $m_{\rm I}$ is the initial mass of each individual star and the slope $\alpha = 2.35$ corresponds to the Salpeter IMF (Salpeter 1955). The normalization factor $M_{s,0}$ is a function of α, $m_{\rm l}$ (lower mass cut-off), and $m_{\rm u}$ (upper mass cut-off). These $m_{\rm l}$ and $m_{\rm u}$ are set to be $0.1{\rm M}_\odot$ and $50{\rm M}_\odot$, respectively (so that the normalization factor $M_{s,0}$ is dependent simply on α). We investigate models with different α to find the model(s) that can best explain the observed abundance patterns of stars in the LMC. We do not discuss models with different $m_{\rm u}$, because the effects of changing $m_{\rm u}$ on the LMC chemical evolution are similar to those of changing α.

As shown in BT12, a steeper IMF ($\alpha = 2.55$) can slightly better explain the observed chemical abundances and gas mass fraction of the LMC than the Salpeter IMF, if stellar wind (from SNe) is not included in the models. Since the main purpose of this paper is to demonstrate the dust wind effects on galactic chemical evolution clearly (not to find the best IMF model), it would be important for this paper to demonstrate that the dust wind effects derived from the Salpeter IMF model can be true for other models with different IMFs, in particular, $\alpha = 2.55$. We thus briefly discuss the dependences of the present results on IMFs in the Appendix B.

Recent numerical simulations have clearly shown that galaxy-scale stellar winds driven by SN explosions can eject a significant amount of ISM out of dwarf galaxies (e.g., Recchi et al. 2013; Ruiz et al. 2013), which implies that the present model assumption of no stellar wind would be less realistic for the LMC. Although BT12 have already investigated the effects of stellar winds on the chemical evolution of the LMC, it would be important for this study to confirm that the dust wind effects on galactic chemical evolution derived from the models with no stellar winds can be true also for the models with stellar winds. Since the detailed investigation of stellar wind effects on galactic chemical evolution is not the major purpose of this paper, we discuss this issue by using a reasonable set of the LMC models with stellar winds in the Appendix C.

2.8 Main points of analysis

2.8.1 Comparison between observations and models

We discuss how dust wind influences chemical evolution of galaxies by comparing the results of the present chemical evolution models with recent observations derived for the LMC. We therefore adopt a reasonable set of model parameters for the LMC (BT12) and thereby investigate the

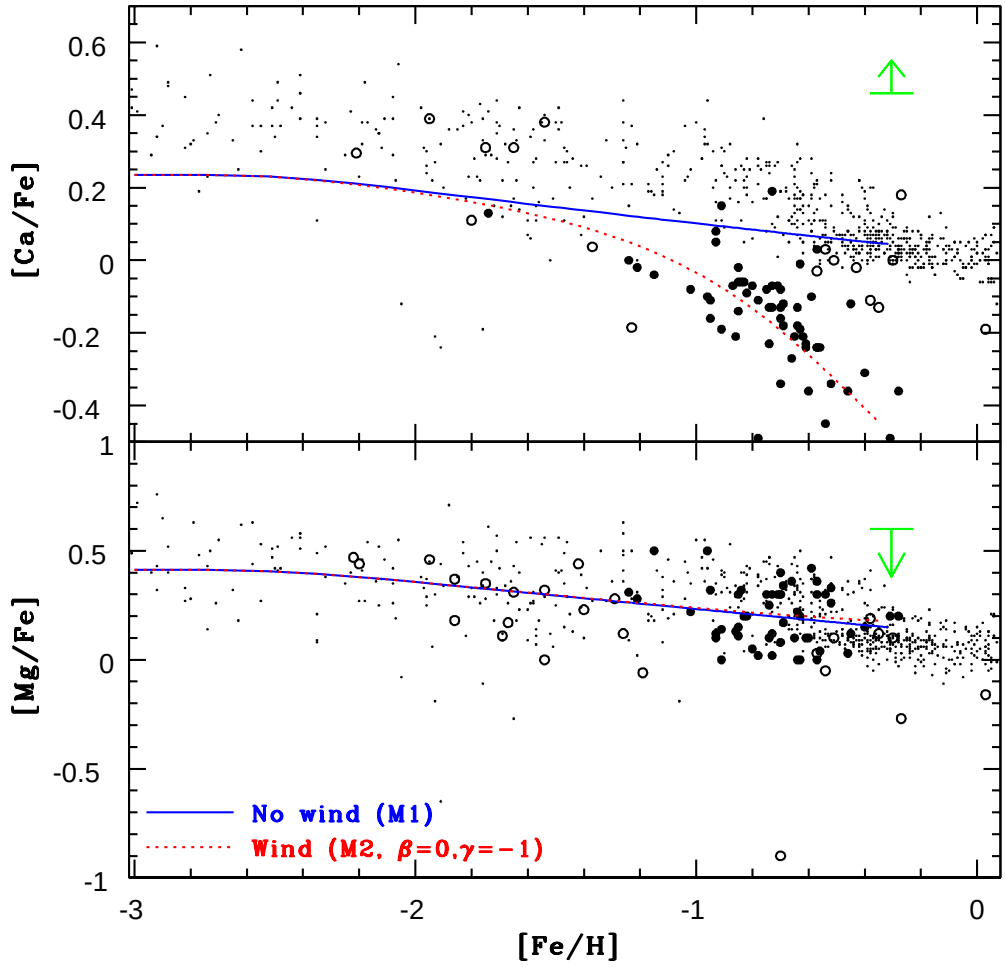

Figure 2. The evolution of [Ca/Fe] (upper) and [Mg/Fe] (lower) as a function of [Fe/H] for the LMC model without dust wind (M1, blue solid) and with dust wind (M2, red dotted). The observed locations of the LMC field stars (big filled circles) and clusters (big open circles) and the Galactic field stars (small dots) on the [Mg/Fe]-[Fe/H] plane are shown for comparison. The observational results include P08 for the LMC field stars, Johnson et al. 2006, Mucciarelli et al. (2008, 2010, 2011), and C12 for the LMC clusters, and Venn et al. (2004) for the Galactic field stars. The green arrows indicate the possible differences in the observed [Ca/Fe] (+0.09 dex) and [Mg/Fe] (−0.22 dex) between P08 and V13 (i.e., the most recent observational study). The higher [Ca/Fe] in V13 implies that if the models are compared with V13, then weaker dust wind is required to reproduce the observed [Ca/Fe] at higher metallicities in the LMC.

time evolution of several selected elements (e.g. Fe, Ca, and Mg). We mainly investigate the LMC because of the two reasons described in §1. Like BT12, we focus on the observational results by P08, which clearly shows intriguing results on the [Ca/Fe]-[Fe/H] and [Mg/Ca]−[Fe/H] relations of the LMC. The unusually low [Ca/Fe] (< -0.3) and high [Mg/Ca] (> 0.3) for stars that are not so metal-poor in P08 were found to be hardly explained by our previous models with a standard set of model parameters for the IMF and the star formation history of the LMC.

However, it should be noted here that the latest results by V13 show a higher [Ca/Fe] (by 0.09 dex) in comparison with P08. This difference between the two observational studies can be seen in other α-elements (e.g., [Mg/Fe] by 0.22 dex), which implies that observational results need to be carefully compared with theoretical ones. These differences suggest that the inconsistency between our previous models (BT12) and observations is not so large in terms of [Ca/Fe]−[Fe/H] and [Mg/Ca]−[Fe/H] relations. In the present study, we still mainly use the results by P08, because we need to compare the previous models in BT12, which failed to explain the results by P08, with the present new one, by using the same observational data sets. This comparison allows us to demonstrate the improvement of the present model over the previous one more clearly. We later discuss whether weaker dust wind is required for explaining the observational results by V13.

2.8.2 Parameter study

We mainly investigate the LMC model (M1-M10) with the Salpeter IMF, $f_{\rm b} = 0.03$ $C_{\rm sf} = 0.006$, $t_{\rm a} = 0.3$ Gyr in the

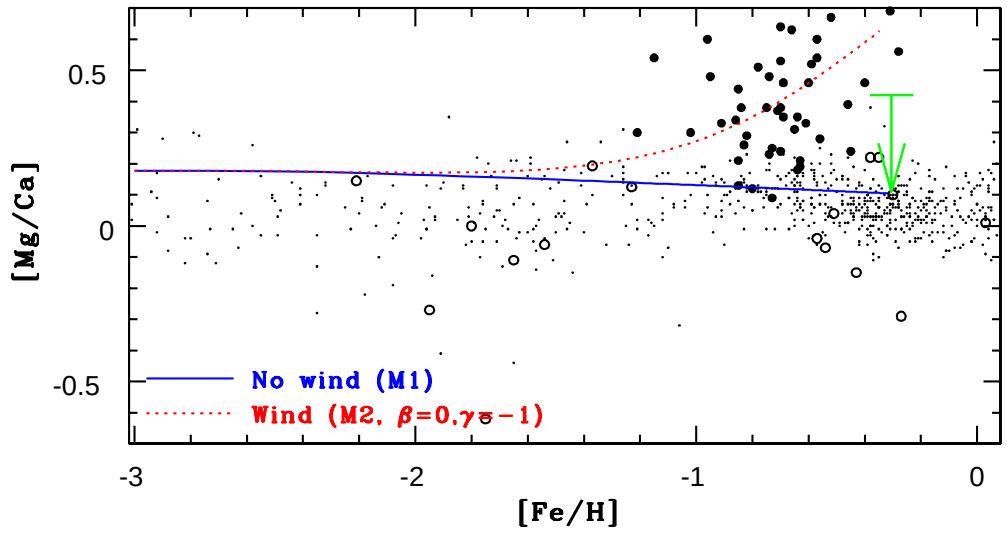

Figure 3. The evolution of [Mg/Ca] as a function of [Fe/H] for the LMC model without dust wind (M1, blue solid) and with dust wind (M2, red dotted). The green arrow indicates the possible difference in the observed [Mg/Ca] (−0.31 dex) between P08 and V13.

present study. We choose these parameter values, because they can better reproduce the age-metallicity relation and chemical abundance patterns in the LMC (BT12). The parameters values for dust wind in these models (β, γ, and $C_{\rm r}$) are different and summarized in Table 2. We do not discuss how the IMF slope and $f_{\rm b}$ influence the chemical evolution of galaxies, because BT12 already discussed these in detail. We also investigate the models that are reasonable for the Fornax dwarf galaxy (F1-F2) and giant elliptical galaxies (E1-E4) in order to discuss the origin of the observed intriguing abundances of these galaxies. Since the results of the LMC are more important than other models (F1-F2 and E1-E4), we first describe the results of the LMC model in §3. We describe the model parameters for the Fornax galaxy and early-type galaxy models and discuss briefly the results of the models in §4. The parameter values for these models are summarized in Table 2.

Once metals are removed from the main body of a galaxy to be located in the halo region through radiation-driven dust wind, the metals can not be returned back to the main body. The two key parameters for this radiation-driven dust (metal) removal process in a galaxy, β and γ, can determine the mass fraction of i-the element (metal) that is removed from the main body of a galaxy ($M_{{\rm halo},i}$) to the total mass of the element in the main body and the halo ($M_{{\rm tot},i}$). The mass fraction ($f_{{\rm dw},i}$) is defined as follows:

$$f_{{\rm dw},i} = \frac{M_{{\rm halo},i}}{M_{{\rm tot},i}}. \quad (13)$$

This 'dust (metal) removal fraction' ($f_{{\rm dw},i}$) evolves with time (t) and can be significantly different between different elements owing to the adopted dependence of P_i on δ_i. In the present model, dust removal means metal removal from the main bodies of galaxies so that higher $f_{{\rm dw},i}$ means that a smaller amount of i-the metal can remain in the main bodies. We investigate how $f_{{\rm dw},i}$ depends on β and γ for a given set of model parameters (e.g., $C_{\rm r}$ and $C_{\rm sf}$).

3 RESULTS

3.1 Evolution of $f_{{\rm dw},i}$

Figure 1 shows how $f_{{\rm dw},i}$ evolves with time for three different elements (Mg, Ca, and Fe) for a given set of dust wind parameters in the LMC models with $C_{\rm r} = 10^{-3}$. In this figure, the higher $f_{{\rm dw},i}$ means a larger mass fraction of the i-the element is removed from the main body of a galaxy. Clearly, Ca is the most efficiently removed from the main bodies of galaxies for all 8 models (M1-M8) with different β and γ. The dust removal fraction of Fe is higher than that of Mg at all time steps in the model M2 with $\beta = 0$ and $\gamma = -1$ that could be the most reasonable in the present study. The dust removal fraction between Fe and Mg can be clearly seen only in the models with $\beta = 0$ and 0.1 for a fixed $\gamma = -1$. The parameter β for a fixed γ can determine the minimum level of dust removal fraction so that larger β can cause the smaller differences in dust removal fraction between the three elements.

The differences in the dust removal fractions of Mg, Ca, and Fe are larger in the models with $\gamma = -0.5$ than those with $\gamma = -0.3$ for a fixed β (0.1 and 0.3). These differences in $f_{{\rm dw},i}$ can cause the different evolution in different elements, as described later. These models all show that the evolution of $f_{{\rm dw},i}$ is rather rapid in the early phase of galaxy evolution ($t < 2$ Gyr) owing to the dramatic luminosity evolution caused by high SFRs. However, the small $f_{{\rm dw},i}$ (i.e., $\log f_{{\rm dw},i} < -1$) in this early-phase means that such dust removal can not so strongly influence the chemical evolution of galaxies. In these LMC models, metals in the main body of galaxies can be removed more slowly yet steadily in the later evolution phase so that $f_{{\rm dw},i}$ can be high (> 0.1)

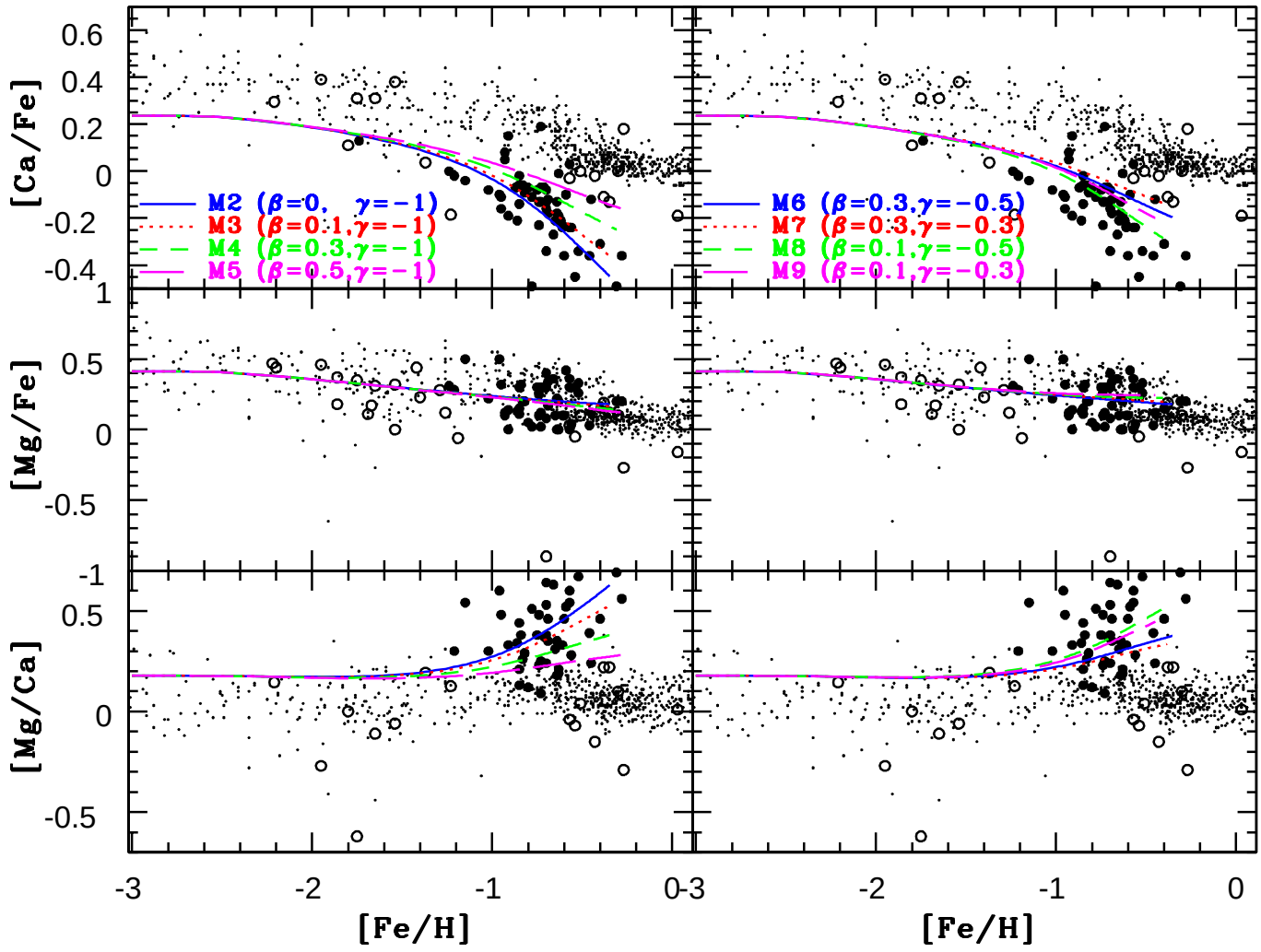

Figure 4. The evolution of [Ca/Fe] (top), [Mg/Fe] (middle), and [Mg/Ca] (bottom) as a function of [Fe/H] for the eight LMC models with different β and γ. In the left three frames, blue, red, green, and magenta lines represent the models with $\beta = 0$ and $\gamma = -1$ (M2), $\beta = 0.1$ and $\gamma = -1$ (M3), $\beta = 0.3$ and $\gamma = -1$ (M4), and $\beta = 0.5$ and $\gamma = -1$ (M5), respectively. In the right three frames, blue, red, green, and magenta lines represent the models with $\beta = 0.3$ and $\gamma = -0.5$ (M6), $\beta = 0.3$ and $\gamma = -0.3$ (M7), $\beta = 0.5$ and $\gamma = -0.5$ (M8), and $\beta = 0.5$ and $\gamma = -0.3$ (M9), respectively.

enough to influence chemical evolution. These results suggest that galactic chemical evolution can be more strongly influenced by dust wind at their later evolution stages when galactic luminosities are high enough to exert strong radiation pressure on dust grains.

3.2 Correlations of [Mg/Fe], [Ca/Fe], [Mg/Ca] with [Fe/H]

Fig. 2 compares the evolution of [Ca/Fe] and [Mg/Fe] as a function of [Fe/H] in the two LMC models with (M2) and without dust wind (M1). Clearly, there is no significant difference in the observed [Mg/Fe]−[Fe/H] relations of the LMC and the MW, though the LMC shows a large [Mg/Fe] scatter for a given [Fe/H] at [Fe/H]> -1, which could be caused by secondary starburst due to tidal interaction with the SMC (BT12). However, the [Ca/Fe]−[Fe/H] relation of the LMC is quite different from that of the MW, in particular, for the higher [Fe/H] (> -1). These observations can not be well reproduced self-consistently by the model M1 without dust wind. The models without dust wind can only explain the observed [Mg/Fe]−[Fe/H] relation of the LMC by adopting a reasonable set of model parameters, but it fails to explain the observed rather low [Ca/Fe] < -0.3 at [Fe/H]> -0.6.

The dust wind (M2) can reproduce both the observed [Mg/Fe]−[Fe/H] and [Ca/Fe]−[Fe/H] relations in a self-consistent manner for $C_{\rm r} = 10^{-3}$, $\beta = 0$, and $\gamma = -1$. As shown in Fig. 1, Ca can be more efficiently removed from the main body of the LMC than Fe through radiation-driven dust wind in this model M2. As a result of this, [Ca/Fe] can decrease more rapidly with increasing [Fe/H] in comparison with the model M1 without dust wind. Since both Mg and Fe are less efficiently removed from the main body of the LMC, their time evolution can not be so strongly influenced by dust wind. Therefore the [Mg/Fe]−[Fe/H] relation is not

so different between the models with and without dust wind. It should be noted here that the apparently larger [Ca/Fe] differences at higher [Fe/H] between the LMC and the MW can be reproduced reasonably well by the dust wind model.

Fig. 3 shows that (i) the observed [Mg/Ca] are rather high (> 0.3) for a sizable fraction of stars in the LMC at [Fe/H]> -1 and (ii) [Mg/Ca] appears to increase with [Fe/H] for the field stars of the LMC at [Fe/H]> -1.2. Clearly, only the dust wind model can reproduce the observed rather high [Mg/Fe] of some stars in the LMC at higher [Fe/H]. The apparent [Mg/Ca] increase with [Fe/H] can be well reproduced by the dust wind model (M2) while the model M1 without dust wind does not show such a trend at all. These results imply that the observed trend is caused by a larger degree of Ca removal through dust wind in the chemical evolution of the LMC. However, the observed [Mg/Ca] dispersion at a given [Fe/H] is quite large, which makes it difficult for the present study to propose a robust physical interpretation of the observed apparent [Mg/Ca] increase with [Fe/H]. It is unclear why the observed [Mg/Fe] ([Ca/Fe]) of clusters in the LMC appear to be smaller (larger) than those of the field stars.

It should be stressed that the observed [Ca/Fe] by V13 is larger by 0.09 dex than P08, which means that the observed [Ca/Fe] at [Fe/H]~ -0.3 is about -0.3 rather than -0.4 in V13. Accordingly, if we adopt the V13 results, then a weaker dust wind that removes a smaller amount of gas-phase metals is required for the consistency of the model with the observation. The possible difference in [Mg/Ca] between P08 and V13 is 0.3 dex, which also suggests that a significantly weaker dust wind is required to explain [Mg/Ca]$\sim$ 0.3 (rather than ~ 0.6) in the present models. Thus the required level of the removal process of Mg and Ca by dust wind to explain the observed [Mg/Ca]$-$[Fe/H] relation can be reduced, if the observed [Ca/Fe] and [Mg/Fe] can be further systematically higher and lower, respectively, in future observational studies.

It should be also noted that [Fe/H] is not so different between the two models with and without dust wind, because gas-phase Fe is not removed so efficiently by dust wind. BT12 suggested that if Fe can be preferentially lost in the LMC through some wind processes, then the observed rather high [Ba/Fe] would be explained , because Ba is less efficiently removed through stellar wind. This implies that the present models with no stellar wind would not reproduce well the observed high [Ba/Fe] in the LMC, even if the time evolution of [Ba/Fe] is investigated.

3.3 Parameter dependences

Fig. 4 compares the [Ca/Fe]$-$[Fe/H], [Mg/Fe]$-$[Fe/H], and [Mg/Ca]$-$[Fe/H] relations between the eight dust wind LMC models (M2-M9) with different β and γ (for a fixed $C_{\rm r}$). There is no substantial difference in the [Mg/Fe]$-$[Fe/H] relations between the dust wind models (M2-M5) with different β for a fixed $\gamma = -1$, because the dust removal fractions of Mg and Ca are not so different for the ranges of these parameters, as shown in Fig. 1. The [Ca/Fe]$-$[Fe/H] and [Mg/Ca]$-$[Fe/H] relations depend on β for a fixed $\gamma = -1$ in such a way that [Ca/Fe] and [Mg/Ca] can be systematically lower and higher, respectively, at a given [Fe/H] for smaller β. The models with smaller β are more consistent with observations among the four models (M2-M5) with a fixed γ in terms of reproducing the observed [Ca/Fe]$-$[Fe/H] and [Mg/Ca]$-$[Fe/H] relations. These results imply that if the observed [Ca/Fe]$-$[Fe/H], [Mg/Fe]$-$[Fe/H], and [Mg/Ca]$-$[Fe/H] relations are all real, then a steeper dependence of P_i on δ_i is required for reproducing these three relations in a self-consistent manner.

The dependences of the three relations on γ for a fixed β are not so remarkable in comparison with those on β (for $-1 \leqslant \gamma \leqslant -0.3$). The models with smaller γ show systematically lower [Ca/Fe] and higher [Mg/Ca] for $\beta = 0.3$ and 0.5, because the $f_{{\rm dw},i}$ difference between Ca, Mg, and Fe is larger for smaller γ. The models with smaller γ for a fixed β can better reproduce the observed [Ca/Fe]$-$[Fe/H], [Mg/Fe]$-$[Fe/H], and [Mg/Ca]$-$[Fe/H] relations in a self-consistent manner. These results confirm that γ needs to be small so as to explain the observed three relations reasonably well. Owing to the observed larger dispersions of [Ca/Fe], [Mg/Fe], and [Mg/Ca] at a given [Fe/H], it is currently impossible for the present study to determine the best set of β and γ for which the three observations can be most self-consistently explained.

3.4 Prediction of lower [Ti/Fe]

Since Ti is the second most severely dust-depleted element next to Ca among the observed elements (e.g., Fig. 4 in SS96), the time evolution of Ti can be influenced by dust wind to a larger extent than Mg and Fe in the present dust wind model. It is therefore useful for the present study to provide some predictions on the [Ti/Fe]$-$[Fe/H] relation of the LMC by using the same LMC models discussed in preceding sections. Fig. 5 shows the clear systematic differences in [Ti/Fe] evolution between the LMC models with and without dust and (ii) the degrees of the [Ti/Fe] differences depend on β and γ. However, the differences are not so large as those derived for [Ca/Fe] and [Mg/Ca], which is expected for a smaller dust removal fraction for Ti. The present study therefore predicts that the LMC shows systematically lower [Ti/Fe] than the MW and the degree of the [Ti/Fe] differences between the LMC and the MW is smaller than that of Ca, if the chemical evolution of the LMC is influenced by dust wind. The results of P08 appear to be consistent with the above predictions, though the observed dispersions of [Ca/Fe] and [Ti/Fe] at a given [Fe/H] are large.

4 DISCUSSION

4.1 The influences of dust sizes on the present results

We have so far focused on the results of the models in which the possible differences in sizes between different dust grains (in particular, Mg- and Ca-bearing ones) are not included. As discussed in §2.1.3, the typical size of Ca-bearing dust can be possibly smaller than that of Mg-bearing one, if Ca-bearing dust can be preferentially formed in SNe. Furthermore, Kozasa & Hasegawa (1987) showed that Ca-bearing dust ($CaTiO_3$) is typically smaller than Mg-bearing one ($MgSiO_3$) in their theoretical models of dust formation in cooling gas of the solar composition (e.g., see their Fig. 2).

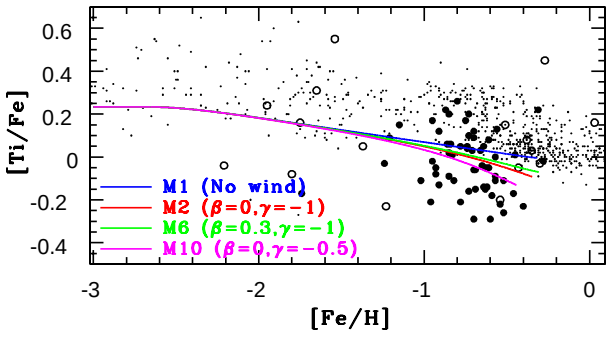

Figure 5. The evolution of [Ti/Fe] as a function of [Fe/H] for the eight LMC model with and without dust wind for different β and γ. Blue, red, green, and magenta lines represent the models with no dust wind (M1), $\beta = 0$ and $\gamma = -1$ (M2), $\beta = 0.3$ and $\gamma = -1$ (M6), $\beta = 0$ and $\gamma = -1$ (M10), respectively.

F91 clearly showed that only a factor of two difference in dust sizes (silicate vs graphite in their model, see their Fig 7) can cause a significant difference in the time evolution of the dust removal processes. Given that dust with smaller sizes can be more efficiently removed from galaxies (F91), Ca-bearing dust with its possibly smaller size would be likely to be removed even more efficiently than the present study derived. Thus, the present results (which depend on more efficient removal of Ca than Mg) can not be qualitatively changed by including the possible size differences between Mg- and Ca-bearing dust, if Ca-bearing dust has a smaller size than Mg-bearing one.

However, if the typical size of Mg-bearing dust is significantly (by more than a factor of two) smaller than that of Ca-bearing one, then the present results can be changed qualitatively, because Mg-bearing dust can be more efficiently removed from galaxies than Ca (even if the depletion level of Mg is lower than that of Ca). We can not currently make a quantitative estimation on the typical sizes of Mg- and Ca-bearing dust owing to the lack of extensive observational and theoretical works on the sizes of these dust. Furthermore, there is no detailed theoretical work how P_i, which determines the dust removal efficiency, depends on physical properties of dust in ISM such as dust sizes and compositions. Therefore, it is reasonable for the present study to suggest that the present results could be changed if the influences of the typical sizes of Mg- can Ca-bearing on dust removal efficiencies are properly modeled. If future theoretical studies on the typical sizes of Ca-bearing dust in SNe and AGB stars provide a table for the sizes, we will be able to discuss the influences of dust size on the present results in a much more quantitative manner.

4.2 Are there any other explanations for high [Mg/Ca] ?

The present study has shown, for the first time, that both the observed rather high [Mg/Ca] (> 0.3) and the increasing trend of [Mg/Ca] with increasing [Fe/H] (at [Fe/H]> -1) in the LMC can be self-consistently reproduced by the dust wind model for a reasonable set of the model parameters. Although this can be regarded as remarkable improvement of our chemical evolution model over BT12, it should be

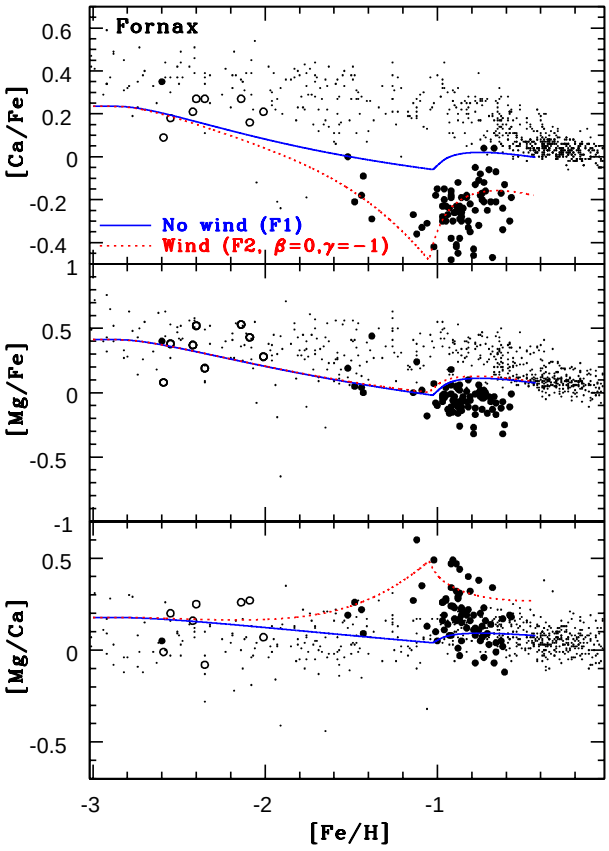

Figure 6. The evolution of [Ca/Fe] (top), [Mg/Fe] (middle), and [Mg/Ca] (bottom) as a function of [Fe/H] for the two Fornax models without dust wind (F1, blue solid) and with dust wind (F2, red dotted). In these Fornax models, a secondary starburst with a high SFR at $t = 5$ Gyr is assumed. The observational results shown for the MW are exactly the same as those in Fig. 2. The results for clusters (big open circles) and field stars (big filled circles) in the Fornax dwarf galaxy from Letarte et al. (2010) are plotted in this figure.

noted that there could be alternative explanations for the observed high [Mg/Ca]. Since different IMFs and selective SN winds can not self-consistently explain the observed [Mg/Fe]−[Fe/H] and [Ca/Fe]−[Fe/H] relations, we consider the following two alternative explanations to the dust wind one.

One is that P08 could overestimate the [Mg/Ca] of stars in the LMC for some reasons. This seems to be the case, given that [Ca/Fe] and [Mg/Fe] derived by V13 for the LMC inner disk and bar are higher and lower, respectively, than those by P08. The reason for this difference between P08 and V13 is that they adopted different stellar parameters and methods to derive stellar abundances. If the abundance determination by V13 is more accurate, then the observed [Mg/Ca] in P08 can be lowered by ~ 0.3 dex and thus become closer to the solar value for most of the investigated stars in the LMC. However, this possible 0.3 dex reduction of [Mg/Ca] is not enough to explain the observed high [Mg/Ca] (> 0.4) of some stars in P08.

The other is that high [Mg/Ca] is due to the contribution of jet-induced SNe that have characteristic nucleosynthesis yields. Using chemodynamical models with explosions

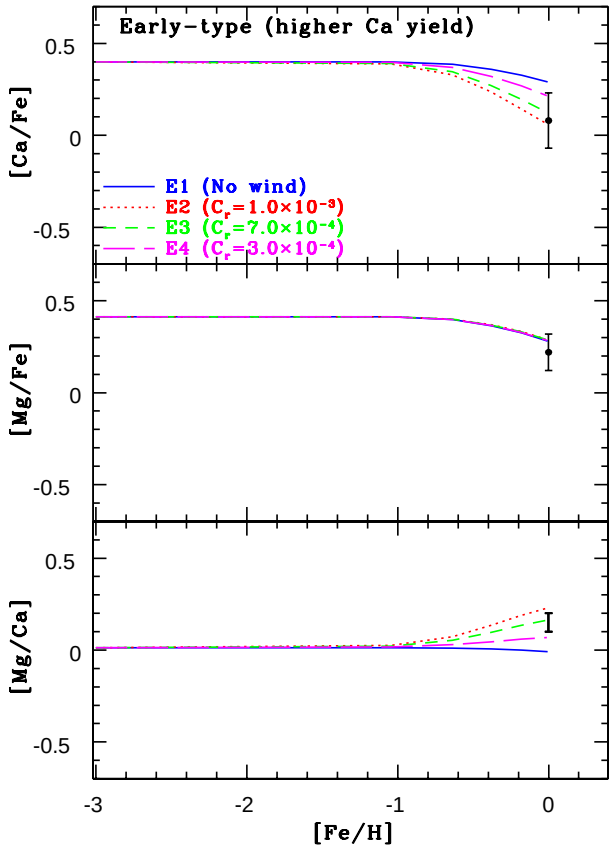

Figure 7. The evolution of [Ca/Fe] (top), [Mg/Fe] (middle), and [Mg/Ca] (bottom) as a function of [Fe/H] for the four early-type models with and without dust wind for different $C_{\rm p}$ (but fixed $\beta = 0$ and $\gamma = -1$). Blue, red, green, and magenta lines represent the models with no dust wind (E1), $C_{\rm r} = 10^{-3}$ (E2), $C_{\rm r} = 7 \times 10^{-4}$ (E3), and $C_{\rm r} = 3 \times 10^{-4}$ (E4), respectively. The observational data for mean values of [Ca/Fe] and [Mg/Fe] (for [Fe/H]$= 0$) from J12 are plotted with an observational error bar (0.1 and 0.15 dex) in the top and middle panels. The observed range of [Mg/Ca] is shown in the bottom panel. For these early-type models, higher Ca yield is used so that both initial [Mg/Fe] and [Ca/Fe] can be as high as those (~ 0.4) of the old Galactic halo stars.

of aspherical SNe (A-SNe), Bekki et al. (2013) investigated how the characteristic chemical yields of A-SNe can influence the chemical evolution of dwarf galaxies. They found that [Mg/Ca] can be quite diverse in different stars for a given [Fe/H] with some stars having as large as [Mg/Ca]~ 0.5: The physical reason for this is discussed in their paper. Although their results imply that the observed rather high [Mg/Ca] in the LMC can be due to the contribution of A-SNe to the chemical evolution, they could not explain the increasing trend of [Mg/Ca] with increasing [Fe/H] in their models. Therefore, the A-SN scenario can not explain both the observed high [Mg/Ca] and [Mg/Ca]$-$[Fe/H] relation of the LMC.

Thus, the dust wind scenario appears to be more promising than the above A-SNe scenario. The dust wind scenario predicts that dust abundance patterns and compositions in outer gaseous halos of galaxies, where interstellar dust can reach owing to radiation pressure of stars under some physical conditions (F91), should be different from those in the main bodies of the host galaxies. For example, the Ca-abundance of dust in gaseous halos could be significantly higher than that in ISM of disks owing to the differential removal process of dust. Therefore, such predictions need to be investigated by observational studies of dust abundances and compositions of gaseous halos of galaxies so that the viability of the scenario can be assessed in a convincing way. Recent observational studies of extinction curves for different halo regions of the Galaxy (e.g., Peek et al. 2013) would provide some information on how the dust abundances and compositions of the halo are different from those of the disk.

4.3 Differential dust removal in other galaxies ?

4.3.1 The MW

As shown in Figs. 2 and 3, the MW does not show low [Ca/Fe] and high [Mg/Ca] for the same metallicity range of the LMC stars. This striking contrast in the [Ca/Fe]$-$[Fe/H] and [Mg/Ca]-[Fe/H] relations between the two galaxies can be understood in the context of the different dust removal efficiencies between the two as follows. Although dust can be possibly removed once from the main disk of the MW through dust wind, a large fraction of the dust can be return back to the original disk to participate the further chemical evolution owing to the deep gravitational potential. On the other hand, the LMC dust can not be returned back to its original disk once it is removed through dust wind, because the shallow gravitational potential can not keep it within the inner halo of the LMC. The strong tidal field of the Galaxy could also prevent the once removed dust from returning back to its original disk of the LMC. Thus, the dust removal efficiency can be dramatically different between the LMC and the MW in the sense that the efficiency is much lower in the MW: the chemical evolution of the MW is less likely to be strongly influenced by dust wind. In order to discuss whether this explanation is reasonable and realistic, we will perform numerical simulations of dust wind for galaxies with different gravitational potentials in our future works.

4.3.2 Fornax dwarf galaxy

Recent spectroscopic observations of stars in the Fornax dwarf galaxy (e.g., Letarte et al. 2010) have revealed that [Ca/Fe] at [Fe/H]$\geqslant -1$ is significantly smaller than the solar value while [Mg/Fe] is consistent with the solar value. These trends in the Fornax galaxy are similar to those found for the LMC and summarized in Fig. 6. One of possibly significant differences in the chemical abundance pattern between the LMC and the Fornax galaxy is that [Ca/Fe] decreases with [Fe/H] until [Fe/H]~ -1 and then it appears to start to increase from [Fe/H]~ -1. Below, we briefly discuss whether the dust wind model can explain the observed abundance patterns of the Fornax galaxy. A fully self-consistent chemical evolution model with dust wind for the Fornax galaxy should be constructed in our future paper.

Both recent observational and theoretical studies have shown that the Fornax galaxy could have experienced secondary starbursts possibly triggered by merging of two or

multiple dwarf galaxies (e.g., Coleman et al. 2004; Tsujimoto 2011; Yozin & Bekki 2012; de Boer et al. 2013). Some of recent observational studies have suggested that the starburst events in the Fornax dwarf galaxy can be once between 6 and 9 Gyr ago (e.g., Piatti et al. 2014) and several times in the early formation histories of the galaxy (e.g., Hendricks et al. 2014). Therefore, it is not reasonable for this study to adopt a uniform star formation history without secondary starburst events.

Thus, we consider a one-zone chemical evolution model with a secondary starburst. In this model, the star formation coefficient ($C_{\rm sf}$) can become rather high during the starburst period. We assume that (i) $C_{\rm sf}$ is 0.003 before the starburst and 0.04 after the starburst, (ii) the starburst occurs during t = 5 and 6 Gyr, (iii) SF is truncated after the starburst, and (iv) $f_{\rm b}$, β, γ, and $C_{\rm r}$ are set to be 0.09, 0, -1, and 6×10^{-3}, respectively, in this model. These values of basic model parameters are chosen such that both the observed time evolution of [Ca/Fe] and [Mg/Fe] can be better reproduced. Like the LMC model, these Fornax dwarf models do not include stellar wind from SN explosion for clarity. For comparison, a model with no dust wind yet the same parameter values as those described above is investigated.

Fig. 6 shows that [Ca/Fe] can become rather low (up to -0.5) at [Fe/H]< -1 before the secondary starburst owing to the stronger dust wind assumed in this model. The increasing trend of [Mg/Ca] with increasing [Fe/H] can be clearly seen in the dust wind model, and [Mg/Ca] can be as large as 0.5 at [Fe/H]~ -1. Both [Ca/Fe] and [Mg/Fe] can rapidly increase with the [Ca/Fe] evolution being more remarkable during the secondary starburst so that [Mg/Ca] can finally become smaller ($\sim$ 0.2). The modeled [Mg/Fe] after the starburst is slightly higher than the observed one, which implies that this dust wind model is less consistent with observational results for the Fornax galaxy. However, the wind model implies that radiation-driven dust wind can be responsible for the observed rather low [Ca/Fe] and high [Mg/Ca]. It is interesting to point out that [Ti/Fe] can be slightly larger than [Ca/Fe] for the Fornax galaxy (See Fig. 10 in Letarte et al. 2010) and this trend is consistent with the prediction of the dust wind model. It is our future study to construct a better model to explain both the observed [Mg/Fe] and [Ca/Fe] in the Fornax galaxy.

In the above discussion, it is assumed that the dust removal process is essentially the same between the LMC and the Fornax galaxy, which could be a remnant of dwarf-dwarf merging (i.e., the same model for P_i dependent only on dust depletion levels). It would be possible that dust can be efficiently removed from merging galaxies owing to tidal stripping. Since tidal stripping process does not depend on chemical elements of ISM and phases of ISM (cold or hot), it is unlikely that only a specific type of dust (e.g., Ca-bearing dust) can be preferentially stripped: All of elements would be stripped equally through tidal stripping during merging. Therefore, galaxy merging might not result in differential dust removal required for explaining the observed chemical abundances of the Fornax galaxy.

4.3.3 Early-type galaxies

Thomas et al. (2003, T03) investigated the abundances of various α elements in early-type galaxies and found that Ca abundance is smaller with respect to the other α elements by a factor of $\sim$ 2. They also found that [α/Ca] is larger for early-type galaxies with larger velocity dispersion. Indeed, some of early-type galaxies in Fig. 2 of T03 shows [α/Ca] as large as and larger than 0.1. These results imply that [Mg/Ca] of some early-type galaxies can be higher than the solar value, though the level of [Mg/Ca] enhancement in the galaxies is not so high as that of the LMC. The latest observational results by Johansson et al. (2012, J12) are essentially the same as those in T03, which suggests that the [Mg/Fe] (0.1 $\sim$ 0.2 dex) higher than [Ca/Fe] in T03 is real. J12 derived the relations between the velocity dispersions (σ km s^{-1}) and the chemical abundances (e.g., [Fe/H], [Mg/Fe], and [Ca/Fe]) of elliptical galaxies. These can be used for discussing the origin of [Ca/Fe] and [Mg/Ca] of elliptical galaxies in the present study.

Here we briefly discuss the origin of the higher [Mg/Ca] in early-type galaxies by using the dust wind model in which model parameters can be reasonable for early-type galaxies. In this dust wind model for early-type galaxy formation, $t_{\rm a}$, $t_{\rm end}$, $C_{\rm sf}$, β, and γ are set to be 0.1 Gyr, 0.5 Gyr, 0.6, 0, and -1, respectively. These values of model parameters are chosen such that (i) elliptical galaxies can experience initial massive starbursts and (ii) both final [Fe/H] and [α/Fe] can be high. The stellar wind from SN explosion is not included in these elliptical galaxy models. In these models, Ca yield ($Y_{\rm Ca}$) is higher than the theoretical yield of Ca from T95 ($Y_{\rm Ca,0}$) so that both the initial [Mg/Fe] and [Ca/Fe] can be as high as those of the Galactic old halo stars. The parameter $C_{\rm r}$ is changed so that we can see the dependence of galactic chemical evolution of the strength of radiation pressure on dust grains. For comparison, a model in which dust wind is not included and model parameters are exactly the same as those in the dust wind model is investigated. These models can show the final [Fe/H] and [Mg/Fe] as large as 0 and and 0.2, respectively, which are reasonable for luminous early-type galaxies. Based on the observational results in J12 (their Figs. 9, 11, and 13), we can derive the mean [Mg/Fe], [Ca/Fe], and [Mg/Ca] for [Fe/H]= 0 (i.e., $\log \sigma = 2.2$).

Fig. 7 shows that if $C_{\rm r}$ is as large as 7×10^{-4} (i.e., 70% of the one adopted for the LMC model), then the final [Mg/Ca] can be consistent with the observed range of [Mg/Ca]. Owing to the rather high SFRs thus high radiation pressure on dust in these dust wind models, a significant fraction of Ca can be removed from the main galaxies. The model with no dust wind, on the other hand, shows a lower final [Mg/Ca] ($\sim$ 0). These results imply that the observed higher [Mg/Ca] of some bright elliptical galaxies could be due to the differential dust removal driven by radiation pressure of stars in forming early-type galaxies. The observed mean [Mg/Ca] at [Fe/H]=0 in J12 can be consistent with the model E3 whereas the observed mean [Ca/Fe] is best fit to the model E2-E4 with dust wind. It should be stressed here that Fig. 7 just illustrates one possible scenario for the observed higher [Mg/Ca] in early-type galaxies. There could be other explanations for the observed underabundance of [Ca/Fe] and higher [Mg/Ca], such as metallicity-dependent SN yields (T03), which needs to be explored by our future studies. Thus, the present study suggests that the observed higher [Mg/Ca] in massive dwarfs and early-type galaxies can be explained in terms of radiation-driven dust wind in galaxies.

5 CONCLUSION

We have investigated how radiation-driven dust wind can influence galactic chemical evolution by using our new one-zone chemical evolution models. We have particularly focused on the time evolution of [Fe/H], [Mg/Fe], [Ca/Fe], and [Mg/Ca] in massive dwarf galaxies (e.g., LMC), because these galaxies are observed to have intriguing abundance patterns that were not explained reasonably well by our previous models without dust wind. By comparing between the present new results and the latest observations, we have tried to find how the model parameters for dust wind can control the time evolution of the correlations between [Fe/H], [Mg/Fe], [Ca/Fe], and [Mg/Fe]. Although the adopted dust wind model is somewhat idealized, we have found the following preliminary results.

(1) The time evolution of [Ca/Fe] can be significantly different between the models with and without dust wind in the sense that [Ca/Fe] at a given [Fe/H] is lower in the dust wind model. On the other hand, [Mg/Fe] at a given [Fe/H] is not different between the two models with and without dust wind. This is mainly because Ca is more severely dust-depleted than Mg and Fe so that Ca can be more efficiently removed from galaxies through radiation-driven dust wind. This 'differential dust removal' is the main physical mechanism for the derived different evolution of [Ca/Fe] and [Mg/Fe] in the present models.

(2) As a result of differential dust removal, the time evolution of [Mg/Ca] can be significantly different between the models with and without dust wind. The higher [Mg/Ca] in the dust wind model is more consistent with the observed [Mg/Ca] in the LMC and Fornax. Furthermore, the dust wind model predicts an increasing trend of [Mg/Ca] with [Fe/H], which also appears to be consistent with observations for these massive dwarfs. It should be noted, however, that the observed [Mg/Ca] show a large scatter and the latest observations of [Mg/Ca] have lowered [Mg/Ca] (V13) in comparison with previous observations (P08).

(3) [Ti/Fe]−[Fe/H] relation can be significantly different between the models with and without dust wind. However, the difference is not so large in comparison with the [Ca/Fe]−[Fe/H] relation, because Ti is the second most severely dust-depleted next to Ca among the observed elements. These predicted trends are apparently observed in the inner disk of the LMC and Fornax.

(4) Final [Ca/Fe] and [Mg/Ca] in the early-type galaxy models with dust wind can be lower and higher, respectively, than the models without dust wind. This is mainly because much stronger radiation-driven wind in the initial starburst phases of elliptical galaxy formation can remove their dust quite efficiently. The derived lower [Ca/Fe] and higher [Mg/Ca] can provide a new clue to the origin of the observed [Ca/Fe] and [Mg/Ca] in elliptical galaxies.

(5) The differential dust removal process depends basically on the two parameters, β and γ (which controls the minimum level of the dust removal efficiency and the dependence of the efficiency on the dust depletion level, respectively). For a given β, differences in [Ca/Fe] between models with and without dust wind can be larger for smaller γ (i.e., steeper dependence of dust-removal efficiency on dust-depletion level). For a given γ, the [Ca/Fe] differences between the two models can be larger for smaller β. Although the adopted functional form of $P_{\rm i}$ (depending on β and γ) can be reasonable, these two parameters are currently very hard to be constrained by observations.

(6) These results in (1)-(5) suggest that galactic chemical evolution can be influenced strongly by galactic luminosity evolution, because the radiation-driven dust removal processes in a galaxy, which depend primarily on the luminosity evolution of the galaxy, can reduce the total amount of gas-phase metals in the main body of the galaxy. The results also suggest that we would need to understand how the physical processes of gas-phase metals being locked up in dust grains depend on the compositions and sizes of dust for each individual element in order to model the differential dust removal processes in a more sophisticated way. This is because the time evolution of dust grains under radiation pressure of stars depends on dust compositions and sizes (F91).

(7) If the differential dust removal modeled in the present study is correct, then we predict that the outer gaseous halos of galaxies, where dust wind can reach under some physical conditions, should have different dust abundances and compositions (e.g., higher Ca abundance) in comparison with ISM of disks. Therefore, future observational studies of dust abundances and compositions in the outer halos of galaxies (far beyond the optical disks) will provide a stringent test for the dust wind model proposed in the present study.

6 ACKNOWLEDGMENT

We are grateful to the referee, Mathieu van der Swaelmen, for his constructive and useful comments that improved this paper.

REFERENCES

Aguirre, A., Hernquist, L., Katz, N., Gardner, J., Weinberg, D., 2001, ApJ, 556, L11
Barsella, B., Ferrini, F., Greenberg, J. M., Aiello, S., 1989, A&A, 209, 349
Bekki, K., 2013, MNRAS, 432, 2298
Bekki, K., 2014, submitted to MNRAS
Bekki, K., Tsujimoto, T., 2012, ApJ, 761, 180 (BT12)
Bekki, K., Shigeyama, T., Tsujimoto, T., 2013, MNRAS, 428, L31
Chiao, R. Y., Wickramasinghe, N. C., 1972, MNRAS, 159, 361
Coker, C. T., Thompson, T. A., Martini, P., 2013, ApJ, 778, 79

Coleman, M. G., Da Costa, G. S., Bland-Hawthorn, J., et al. 2004, AJ, 127, 832
Colucci, J. E., Bernstein, R. A., Cameron, S. A., McWilliam, A., 2012, ApJ, 746, 29 (C12)
Davies, J. I., Alton, P., Bianchi, S., Trewhella, M., 1998, MNRAS, 300, 1006
de Boer, T. J. L., Tolstoy, E., Saha, A., Olszewski, E. W., 2013, A&A, 551, 103
Draine, B. T., 2009, Physics of the interstellar and intergalactic medium
Dwek, E. 1998, ApJ, 501, 643
Ferrara, A., Ferrini, F., Barsella, B., & Franco, J. 1991, ApJ, 381, 137 (F91)
Ferrarotti, A. S., & Gail, H.-P., 2005, A&A, 430, 959
Ferrarotti, A. S., & Gail, H.-P., 2006, A&A, 447, 553
Franco, J., Ferrini, F., Barsella, B., & Ferrara, A., 1991, ApJ, 366, 443
Hendricks, B., et al., 2014, ApJ, 785, 102
Holwerda, B. W., Keel, W. C., Williams, B., Dalcanton, J. J., & de Jong, R. S. 2009, AJ, 137, 3000
Haschke, R., Grebel, E. K., & Duffau, S. 2012, AJ, 144, 106
Hirashita, H., 1999, ApJ, 522, 220
Hirashita, H., 2013, in the conference procceding, "The life cycle of dust in the Universe"
Jenkins, E. B. 2009, ApJ, 700, 1299
Johansson, J., Thomas, D., & Maraston, C. 2012, MNRAS, 421, 1908 (J12)
Johnson, J. A., Ivans, I. I., & Stetson, P. B. 2006, ApJ, 640, 801
Kirby, E. N., Cohen, J. G., Smith, G. H., Majewski, S. R., Sohn, S. T., Guhathakurta, P., 2011, ApJ, 727, 79
Kozasa, T., Hasegawa, H., 1987, PThPh, 77, 1402
Lanfranchi, G. A., & Matteucci, F. 2012, A&A, 512, 85
Letarte, B., et al. 2010, A&A, 523, 17
Maoz, D., Sharon, K., & Gal-Yam, A. 2010, ApJ, 722, 1879
Maoz, D., Mannucci, F., Li, W., Filippenko, A. V., Della Valle, M., & Panagia, N. 2011, MNRAS, 412, 1508
Maoz, D., & Badenes, C. 2010, MNRAS, 407, 1314
Matteucci, F., & Francois, P. 1989, MNRAS, 239 885
McKee, C. F., & Ostriker, J. P., 1977, ApJ, 218, 148
McWilliam, A., Wallerstein, G., & Mottini, M. 2013, ApJ, 778, 149
Ménard, B., Scranton, R., Fukugita, M., & Richards, G. 2010, MNRAS, 405, 1025
Mucciarelli, A., Carretta, E., Origlia, L., & Ferraro, F. R. 2008, AJ, 136, 375
Mucciarelli, A., Origlia, L., & Ferraro, F. R. 2010, ApJ, 717, 277 (M10)
Mucciarelli, A., et al. 2011, MNRAS, 413, 837 (M11)
Murray, N., Quataert, E., & Thompson, T. A., 2005, ApJ, 618, 569
Nozawa, T., Kozasa, T., Umeda, H., Maeda, K., & Nomoto, K., 2003, ApJ, 598, 785
Pagel, B. E. J., & Tautvaišiené, G. 1998, MNRAS, 299, 535
Peek, J. E. G., & Schiminovich, D. 2013, ApJ, 771, 68
Piatti, A. E., del Pino, A., Aparicio, A., Hidalgo, S. L., 2014, MNRAS in press (arXiv1406.5911)
Piovan, L., Chiosi, C., Merlin, E., Grassi, T., Tantalo, R., Buonomo, U., Cassara, L. P., 2011, in preprint (arXiv1107.4541)
Pipino, A., Fan, X. L., Matteucci, F., Calura, F., Silva, L., Granato, G., & Maiolino, R. 2011, A&A, 525, 61
Pompéia, L., et al. 2008, A&A, 480, 379 (P08)
Recci, S., Hensler, G., 2013, A&A, 551, 41
Roedere, I. U., & Kirby, E. N. in preprint (arXiv:1403.2733)
Roussel, H., et al. 2010, A&A, 518, L66
Ruiz, L. O., Falceta-Goncalves, D., Lanfranchi, G. A., Caproni, A., 2013, MNRAS, 429, 1437
Salpeter, E. E. 1955, ApJ, 121, 161
Savage, B. D., & Sembach, K. R. 1996, ARA&A 34, 279 (SS96)
Sembach, K. R., et al. 2003, ApJS, 146, 165
Spitzer, L., 1978, Physical Processes in the Interstellar Medium (New York: Wiley).
Thomas, D., Maraston, C., & Bender, R. 2003, MNRAS, 343, 279 (T03)
Totani, T., Morokuma, T., Oda, T., Doi, M., & Yasuda, N. 2008, PASJ, 60, 1327
Tsujimoto, T. 2011, ApJ, 736, 113
Tsujimoto, T., & Bekki, K. 2012, ApJ, 736, 113
Tsujimoto, T., Nomoto, K., Yoshii, Y., Hashimoto, M., Yanagida, S., & Thielemann, F.-K. 1995, MNRAS, 277, 945 (T95)
Van der Swaelmen, M., Hill, V., Primas, F., & Cole, A. A. 2013, A&A, 560, 44
Vazdekis, A., et al., 2010, MNRAS, 404, 1639
Welty, D. E., Hobbs, L. M., Lauroesch, J. T., Morton, D. C., Spitzer, L., York, D. G., 1999, ApJS, 124, 465
Winters, J. M., Fleischer, A. J., Le Bertre, T., Sedlmayr, E., 1997, A&A, 326, 305
Xilouris, E., Alton, P., Alikakos, J., Xilouris, K., Boumis, P., Goudis, C., 2006, ApJ, 651, L107
Yoshida, M., Kawabata, K. S., Ohyama, Y., 2011, PASJ, 63, 493
Yozin, C., Bekki, K., 2012, ApJ, 756. L18
Yozin, C., Bekki, K., 2014, MNRAS, 443, 522

APPENDIX A: DEPENDENCES ON CA YIELD

BT12 and the present study used the same *theoretical* chemical yields shown in T95 for consistency between the two works on the LMC chemical evolution. The predicted [Ca/Fe] at lower metallicity ([Fe/H]< -2) in the present LMC models can be therefore ~ 0.24. The [Ca/Fe] in the early phases of the LMC is not so high as $0.3 \sim 0.4$ observed in the metal-poor halo stars of the Galaxy. One might have a concern that the initially lower [Ca/Fe] could be partly responsible for the present successful LMC models reproducing the observed very low [Ca/Fe]. In order to remove this concern, we have investigated the models with higher Ca yields for which the initial [Ca/Fe] can be as high as $0.3 \sim 0.4$.

Fig. A1 shows that for the model with $Y_{\rm ca} = 1.16 Y_{\rm Ca,0}$, the observed low [Ca/Fe] can be well reproduced by adopting slightly higher $C_{\rm r}$ corresponding to a more efficient dust removal process from the main body of the LMC. This result can be seen in the model with $Y_{\rm ca} = 1.46 Y_{\rm Ca,0}$, which means that the essential influences of the dust wind on the LMC chemical evolution do not depend on the adopted Ca yield. These results therefore strengthen the present most important conclusion that the dust wind can be primarily

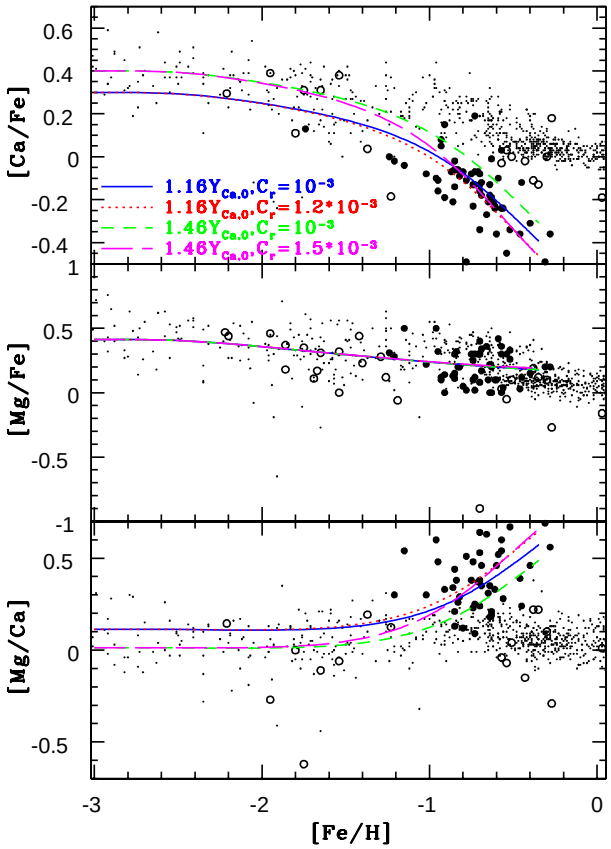

Figure A1. The same as Fig. 4 but for only four models with different Ca yield ($Y_{\rm Ca}$) and $C_{\rm r}$. The theoretical yield of Ca from T95 is referred to as $Y_{\rm Ca,0}$ for convenience. The blue, red, green, and magenta lines represent the models with $Y_{\rm Ca} = 1.16Y_{\rm Ca,0}$ and $C_{\rm r} = 10^{-3}$, $Y_{\rm Ca} = 1.16Y_{\rm Ca,0}$ and $C_{\rm r} = 1.2 \times 10^{-3}$, $Y_{\rm Ca} = 1.46Y_{\rm Ca,0}$ and $C_{\rm r} = 10^{-3}$, and $Y_{\rm Ca} = 1.46Y_{\rm Ca,0}$ and $C_{\rm r} = 1.5 \times 10^{-3}$, respectively. For higher Ca yields, more efficient dust removal (corresponding to larger $C_{\rm r}$) is required for explaining the observed very low [Ca/Fe].

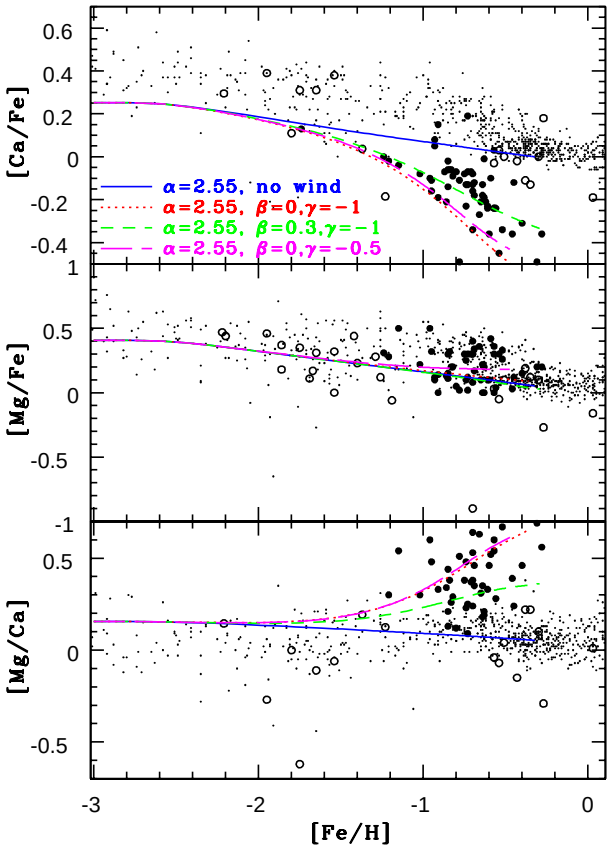

Figure B1. The same as Fig. 4 but for only four models with a same steeper IMF ($\alpha = 2.55$) yet different β and γ. The blue, red, green, and magenta lines represent the models with no dust wind, $\beta = 0$ and $\gamma = -1$, $\beta = 0.3$ and $\gamma = -1$, and $\beta = 0$ and $\gamma = -0.5$, respectively.

responsible for the origin of low [Ca/Fe] and high [Mg/Ca] in the LMC.

APPENDIX B: THE CASE OF A STEEPER IMF

Fig. B1 shows how dust wind can influence the chemical evolution of the LMC in the models with a steeper IMF ($\alpha = 2.55$). In these models, the value of $C_{\rm sf}$ is set to be 0.01 (instead of 0.006 adopted for $\alpha = 2.35$), because final [Fe/H] can be as high as -0.3 owing to the higher SFRs and chemical enrichment processes for such an adoption of $C_{\rm sf}$. Clearly, the models with dust wind can much better reproduce the observed chemical abundances than the model with no dust wind. This strongly suggests that the roles of dust wind in galactic chemical evolution do not depend on the adopted IMFs. Furthermore, these steeper IMF models with dust wind show systematically lower [Ca/Fe] for a given set of β and γ. This results is not so surprising, because our previous models (BT12) have already shown that IMF slopes can control the time evolution of [Ca/Fe]. The dust wind model with $\beta = 0.3$ and $\gamma = -1$ (i.e., smaller difference in dust removal efficiency between Ca and Mg owing to the larger β) can show the highest [Ca/Fe] and the lowest [Mg/Ca] in these models with dust wind.

APPENDIX C: THE ROLES OF STELLAR WINDS IN CHEMICAL EVOLUTION

Fig. C1 show the time evolution of chemical abundances of the LMC in the models with stellar wind ($\alpha = 2.35$). As assumed in BT12, 40% of ejecta from SNII and SNIa is removed completely from ISM of the LMC (i.e., never returned back to original ISM) in these models. This is a 'selective wind' model in the sense that only SN ejecta can be removed from ISM (BT12). The value of $C_{\rm sf}$ is set to be 0.01 (instead of 0.006 adopted for the model with no stellar wind and $\alpha = 2.35$) in these models. This is because final [Fe/H] can not be as high as -0.3 owing to the loss of metals through SN wind, if $C_{\rm sf} = 0.006$ is assumed. The adopted larger $C_{\rm sf}$ results in higher SFRs and thus more efficient chemical enrichment processes so that the final [Fe/H] can be similar to the observed value.

The roles of dust wind in the chemical evolution of the LMC can be clearly seen in these four models with stellar wind. This result can strengthen the present key conclusion that more efficient removal of Ca (in comparison of Mg)

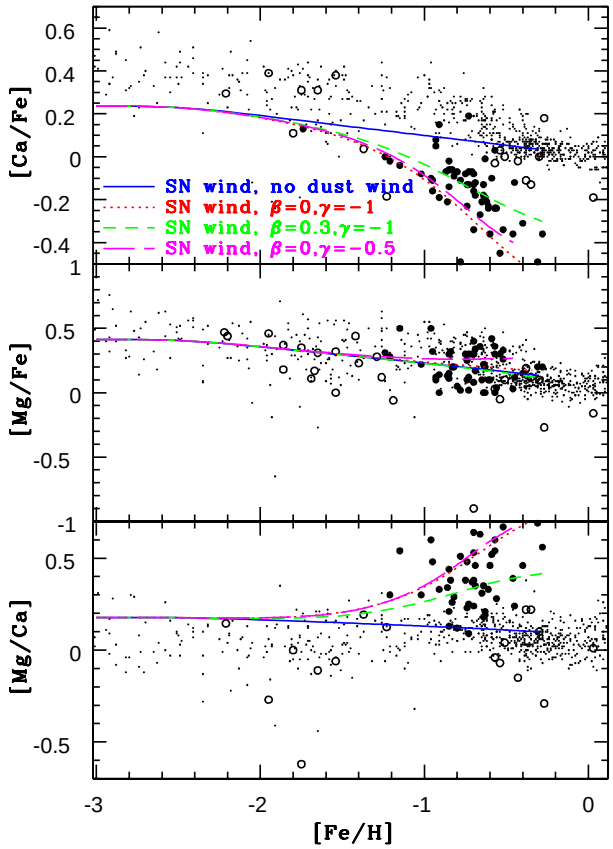

Figure C1. The same as Fig. 4 but for only four models with the Salpeter IMF, stellar wind from SN explosions ('SN wind'), and different β and γ. The blue, red, green, and magenta lines represent the models with no dust wind, $\beta = 0$ and $\gamma = -1$, $\beta = 0.3$ and $\gamma = -1$, and $\beta = 0$ and $\gamma = -0.5$, respectively. In these models with stellar wind, the 'selective wind model' adopted by BT12, in which only SN ejecta can be removed from the LMC through wind, is adopted.

can be responsible for the observed low [Ca/Fe] and high [Mg/Ca] in the LMC. The dependences of the chemical evolution of [Ca/Fe], [Mg/Fe], and [Mg/Ca] on β and γ are essentially the same as those derived in other models. The model with a steeper dependence of P_i on dust depletion levels ($\beta = 0$ and $\gamma = -1$) shows rather low [Ca/Fe] and high [Mg/Ca] in these wind models.